APPLICATION OF AUTOMATED DAMAGE DETECTION OF BUILDINGS DUE TO EARTHQUAKES BY PANCHROMATIC TELEVISION IMAGES

H. Mitomi[1], M. Matsuoka[2] and F. Yamazaki[3]

ABSTRACT

The characteristics of collapsed buildings are examined by image processing of aerial television images taken after the 1995 Hyogoken-Nanbu (Kobe) earthquake. In image processing, not only variance and predominant direction of edge intensity, but also some statistical textures derived from the co-occurrence matrix of edge intensity are used for the extraction of the characteristics of collapsed buildings. The proposed automated damage detection method is applicable to high-resolution satellite imagery such as IKONOS with a panchromatic one-meter spatial resolution as well as to aerial imagery. Using this approach, collapsed buildings in the Kobe images are approximately identified.

Introduction

It is important to grasp damage information in stricken areas just after an earthquake in order to perform quick rescue and recovery activities. Airborne remote sensing is one of the techniques available for gaining disaster information at an early stage, because these images can be obtained quickly with very high resolution. Recently, a new overlay method between pre- and post-event images based on artificial neural networks was applied to detect natural disasters using aerial photographs (Kosugi et al. 2000). However, it is not realistically possible to obtain images of the stricken areas before the disaster. Therefore, we are studying a method of automated detection of damaged buildings due to earthquakes using only post-event images in order to make use of the instantaneous acquisition ability of helicopters and airplanes (Aoki et al. 2001, Mitomi et al. 2001). In our previous study, severely damaged buildings were identified by color indices and edge elements in an original RGB image. However, it was difficult to apply the same threshold values used for color indices to other images, because of the differences in factors such as the influence of sunshine and built environments (Mitomi et al. 2000). In this study, we propose a method of detecting areas with building damage based only on edge information. The application of the method that does not use color information to other aerial images and some panchromatic satellite images, such as IKONOS, QuickBird and OrbView, which have one-meter spatial resolution on the ground surface, can be expected (Gruen 2000).

[1]Earthquake Disaster Mitigation Research Center, NIED, Miki City, Hyogo, Japan 673-0433
[2]Deputy Team Leader, Earthquake Disaster Mitigation Research Center, NIED, Miki City, Hyogo, Japan 673-0433
[3]Team Leader, Earthquake Disaster Mitigation Research Center, NIED, Miki City, Hyogo, Japan 673-0433

Aerial HDTV Images and Training Data

Aerial shooting from helicopters of areas affected by the Kobe earthquake was performed shortly after the event by the Japan Broadcasting Corporation (NHK). These images were taken at a 30-45 degree angle from the vertical direction, from a height of about 300m using NHK's HDTV cameras. In this study, we used some of these images taken 10 days after the event. The HDTV images were converted to RGB image data with a bitmap format, and the panchromatic images were fabricated from the method to obtain the brightness signal for NTSC, which is one of the image transmitting systems used for television. One of the images used in this study is shown in Figure 1. The spatial resolution of this image is approximately 9cm to17cm for near to far distances from the camera, respectively.

Figure 1. Aerial HDTV image.

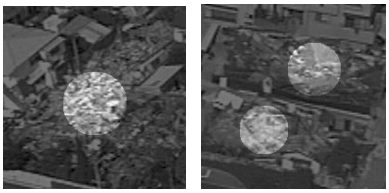

Figure 2. Samples of training data for collapsed buildings.

Table 1. Training data used in this study, and extraction accuracy in cases of both pixel level (*Dpx*) and spatial filtering level (*Darea*).

training data		Dpx (%)			Darea (%)		
		*1	*2	*3	*1	*2	*3
c1	debris of collapsed wooden buildings	45.7	49.3	47.2	90.2	95.5	93.6
c2	brown roof of non-damaged low-rise buildings	0.0	0.0	0.1	0.0	0.0	0.0
c3	gray roof of non-damaged low-rise buildings	0.2	0.4	0.3	0.0	0.0	0.0
c4	big roof of a gymnasium	0.0	0.0	0.0	0.0	0.0	0.0
c5	brown wall of non-damaged low-rise buildings	16.8	19.1	19.1	1.0	2.4	2.6
c6	white wall of non-damaged low-rise buildings	18.6	19.8	19.9	0.0	0.0	0.0
c7	blue vinyl canvas sheets	8.2	9.2	9.4	0.0	0.0	0.0
c8	railways	2.1	2.7	2.5	0.0	0.0	0.0
c9	asphalt roads and parking lots	8.2	9.3	9.3	2.8	5.3	4.4
c10	bare ground	4.4	4.9	5.1	0.0	0.0	0.0
c11	tennis court	1.5	1.6	1.6	0.0	0.0	0.0
c12	vegetation	0.9	1.2	0.9	1.0	1.9	1.4

*1 denotes the combination with four threshold values of Ev, Ed, Ta and Te.
*2 denotes the combination with three threshold values of Ev, Ed and Ta.
*3 denotes the combination with three threshold values of Ev, Ed and Te.

The outlines of undamaged buildings were clearly observed in the images while the images of collapsed buildings were vague due to the preserve of building debris, e.g., roof tiles, soil under the roof tiles and exterior walls. Hence, in this study, the characteristics of the area with collapsed buildings were examined using edge information. Typical areas with collapsed buildings (c1), elements of undamaged buildings (c2-c6), and objects other than buildings (c7-c12) were selected from the aerial image as listed in Table 1. These training data were designated as the areas of inscribed circles. Figure 2 shows samples of training data for the collapsed buildings.

Edge Intensity, Its Variance and Direction

Edge intensity (*Ei*), its variance (*Ev*) and a ratio of predominant direction of edge intensity (*Ed*) were derived from a Prewitt filter, to detect the change in density among neighboring pixels. The Prewitt filter used to detect edge elements has 3x3 matrices, and can calculate edge intensities of eight directions (Takagi and Shimoda 1991). We enlarged this filter to a 7x7 matrix (Aoki et al. 2001), because densities of neighboring pixels have gentle slopes in images taken by television cameras. *Ei* was obtained from the maximum value in the templates for eight directions on edge. An edge direction was defined as the direction of *Ei*, such as 0-180, 45-225, 90-270, and 135-315 degrees. Using the *Ei* value, *Ev* was calculated as a variance in a

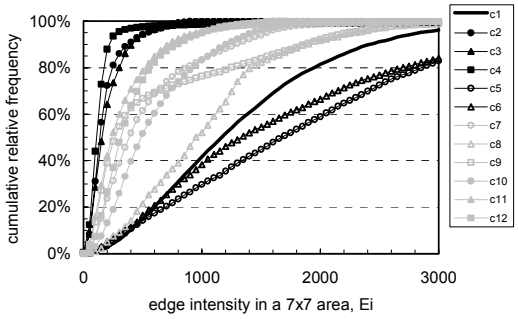

Figure 3. Cumulative relative frequency of *Ei* for training data.

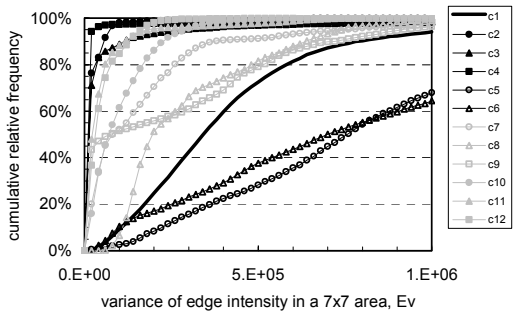

Figure 4. Cumulative relative frequency of *Ev* for training data.

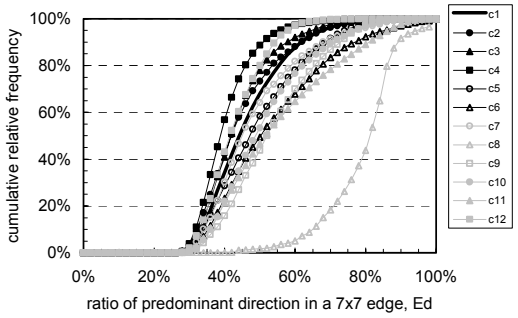

Figure 5. Cumulative relative frequency of *Ed* for training data.

7x7 pixel window. Also, the ratio of the predominant direction of edge elements in a 7x7 pixel window, *Ed*, was calculated. Figures 3, 4 and 5 show cumulative relative frequencies of *Ei*, *Ev* and *Ed*, respectively, for each set of training data. The roofs of undamaged buildings, (c2-c4) including many of the non-edge areas, consist of extremely small values of *Ei* and *Ev*. The exterior walls of undamaged buildings (c5, c6) have stronger edge elements than other training data, due to attachments such as balconies, windows, and outlines of buildings. The distribution of *Ed* of railways (c8) has more pixels with the same edge direction than other training data. In the case of collapsed buildings (c1), the distributions of the values for *Ei* and *Ev* are broad, and the distribution of the value for *Ed* is similar to that of other training data, excepting railways.

Statistical Textures due to Co-occurrence Matrix

An occurrence probability $P(k, l)$ means the probability that pixel value l appears in a relative position $\delta=(r, \theta)$ from a reference pixel whose value is k, where r and θ of δ are relative distance and direction from the reference pixel, respectively. The occurrence probability $P(k, l)$ is calculated for all combinations of pixel values (k, l) against some constant δ. This matrix is called a co-occurrence matrix (Takagi and Shimoda 1991), because column k line l in the matrix represents a co-occurrence probability of pixel values (k, l). Some of the textures due to the co-occurrence matrix are often used to classify land cover in urban areas (Zhang et al. 2001). In this study, characteristics of the collapsed buildings were investigated with edge textures derived from a co-occurrence matrix based on edge intensity, *Ei*. The cumulative relative frequency of the collapsed buildings (c1) was converted to 4-bit data representing a condensed edge intensity, *cEi*, as shown in Figure 6. Figure 7 shows relative frequencies for representative training data. By this approach, the same number of pixels for the collapsed buildings in *cEi* was obtained in all digital numbers of 4bits. On the other hand, exterior walls (c5, c6) have strong elements in *cEi*, and some of the other training data, such as blue vinyl canvas sheets (c7), asphalt roads and parking lots (c9), and bare ground (c10) contain many weak elements in *cEi*. Using these characteristics, two textures were calculated for the condition of r=1, which indicates neighboring pixels around a reference pixel, and four directions of 0-180, 45-225, 90-270, and 135-315 degrees. Figure 8 is a schematic diagram representing the relationship between

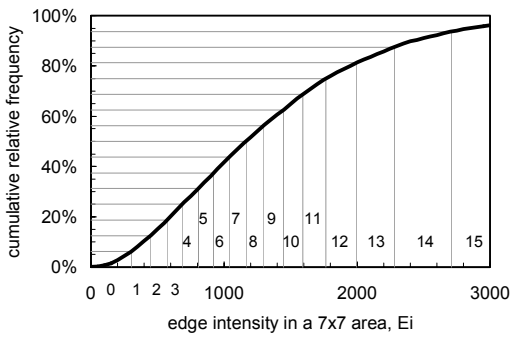

Figure 6. Cumulative relative frequency of *Ei* for the collapsed buildings, and derivation of *cEi* with 16 grades.

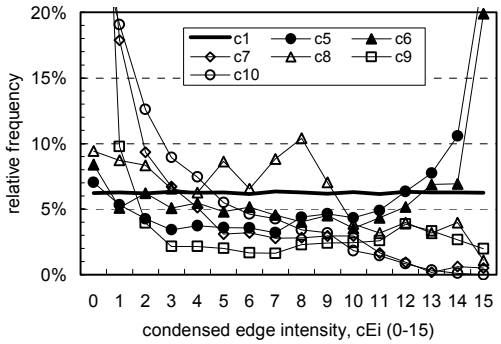

Figure 7. Relative frequency of c*Ei* for some training data.

the reference pixel and other neighboring pixels of distance *r* and direction θ from the pixel. The maximum value for the directions was defined as a representative value of the texture. In addition, a 7x7 pixel area was used as the window size for the texture analysis.

$$Ta = \sum_{k=0}^{m-1}\sum_{l=0}^{m-1}\{P(k,l)\}^2 \tag{1}$$

$$Te = -\sum_{k=0}^{m-1}\sum_{l=0}^{m-1}P(k,l)\log\{P(k,l)\} \tag{2}$$

Equations (1) and (2) describe the angular second moment (*Ta*) and entropy (*Te*) of textures, respectively. Both textures represent the uniformity of the edge structure in the input panchromatic image, but their trends are opposite. If *P*(*k, l*) is locally large in the matrix, which represents uniform texture, large and small values of *Ta* and *Te* are obtained, respectively. As mentioned above, training data of the collapsed buildings should consist of the approximately same number of pixels among each 16 grades for *cEi*. Therefore, it can be expected that the collapsed buildings have non-uniform textures as expressed by *Ta* and *Te*. Figures 9 and 10 show cumulative relative frequencies of each set of training data for *Ta* and *Te*, respectively. The

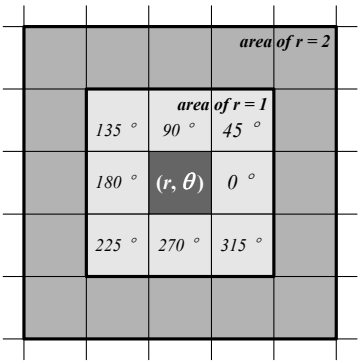

Figure 8. Relationship between a reference pixel and neighboring pixels with *r*=1 and eight directions.

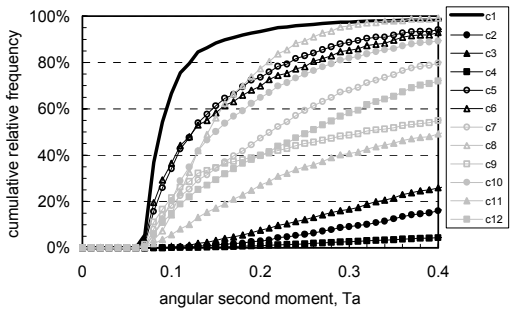

Figure 9. Cumulative relative frequency of *Ta* for training data.

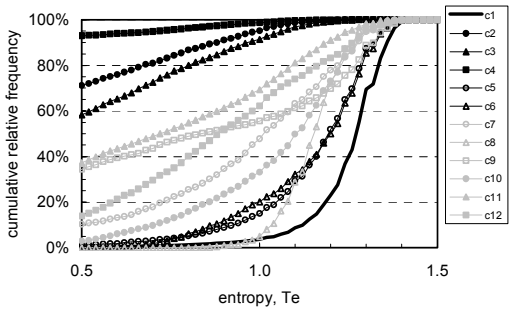

Figure 10. Cumulative relative frequency of *Te* for training data.

collapsed buildings have a large number of pixels representing the lowest range for *Ta* and the highest range for *Te*, respectively. This means the collapsed buildings show the strongest trends of non-uniformity. A slight tendency of non-uniformity is also seen for the exterior walls, railways and bare ground. Most roofs (c2-c4) have a uniform component for the edge structure.

Extraction of Pixels of Collapsed Buildings

The curve of each cumulative relative frequency for the collapsed buildings (c1) shown in Figs 3, 4, 5, 9 and 10 was approximated by a regression line based on the cumulative data between 20% and 80% of the collapsed buildings. If this line intersected 0% and 100% on the graph of the cumulative relative frequency, the threshold value was determined to be the value at these intersection points for each characteristic (Aoki 2001). When each threshold value for *Ei*, *Ev*, *Ed*, *Ta* and *Te* was applied, a ratio of pixels extracted as the collapsed buildings in each training data was attained as shown in Figure 11. In both cases of *Ei* and *Ev*, most of the pixels of

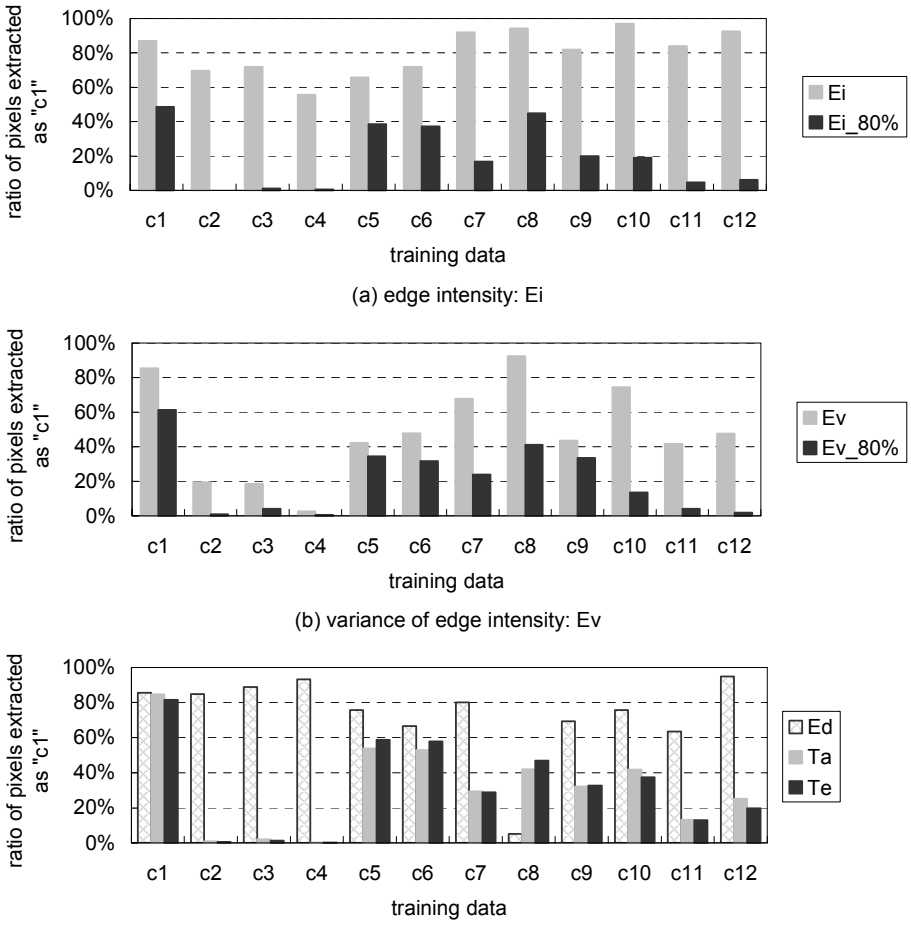

Figure 11. Ratio of pixels extracted for collapsed buildings in each set of training data.

not only the collapsed buildings but also several sets of training data were extracted, in particular, each percentage of pixels extracted as collapsed buildings in blue vinyl canvas sheets (c7), railways (c8), asphalt roads and parking lots (c9) and woods (c12) exceeded that of the collapsed buildings for *Ei*. Railways were clearly distinguished from the collapsed buildings by *Ed*. Using each threshold value of *Ta* and *Te*, about 40% of the pixels consisting of bare ground were extracted, while the ratio of blue vinyl canvas sheets was about 30%. The each value of *Ei* and *Ev*, when cumulative relative frequency for the bare ground (c10) reached 80% in *Ei* and *Ev*, was considered as the lower limit of threshold value in *Ei* and *Ev*, in order to decrease the ratio of extracted pixels of bare ground, as shown in Figs. 3 and 4. On the whole, pixels extracted in the training data, except for the collapsed buildings, decreased in comparison with the result obtained by the threshold values, which were determined by regression lines of the cumulative relative frequencies. Extracted pixels for the roofs of undamaged buildings (c2-c4) disappeared, and those on the bare ground and blue vinyl canvas sheets decreased significantly. However, percentages of correctly extracted pixels for the collapsed buildings also decreased from 86.9% to 48.7% for *Ei*, and from 85.4% to 61.4% for *Ev*. Therefore, *Ei* was not used, but *Ev* with a constrained lower limit of threshold value was used as the parameter to detect building damage. Table 2 shows the threshold values for all parameters used in this study. Pixels within the ranges of all threshold values were regarded as corresponding to building damage.

In this study, accuracies of pixels extracted in combination with not only *EvEdTaTe* but also *EvEdTa* and *EvEdTe*, were evaluated by *Dpx*, as shown in Table 1. *Dpx* is defined as a percentage of extracted pixels in each set of training data, and *Dpx* of the collapsed buildings was between 45% and 50% for the three combinations. Figure 12 shows the transitions of the ratio of the extracted pixels in representative training data when four threshold values were combined in the order of *Ev*, *Ed*, *Ta* and *Te*. Based on *Ev*, it was difficult for the collapsed buildings to be distinguished from other objects, such as exterior walls (c5, c6), railways, asphalt roads and parking lots, and the bare ground. However, the ratios of the number of pixels extracted as collapsed buildings for the other training data, which are not shown in Fig.12, could be

Table 2. Threshold values.

characteristics	threshold
Ev: edge variance	2.0×10^5 - 6.8×10^5
Ed: edge direction	0.30 - 0.60
Ta: angular second moment	0.05 - 0.13
Te: entropy	1.16 - 1.38

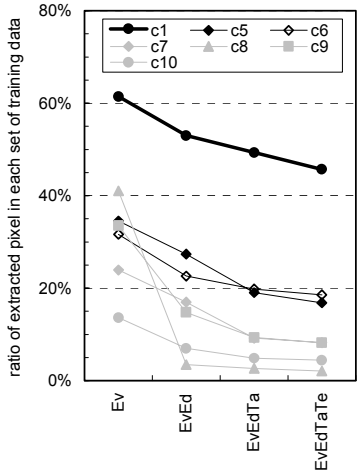

Figure 12. Changes of ratios of *Ev*, *Ed*, *Ta* and *Te* of extracted pixels in some training data.

decreased to less than 5%. Adding the condition of *Ed*, railways were distinguished from the collapsed buildings, because the cumulative relative frequency of *Ed* was significantly different from the other imaged objects, as mentioned above. By using *Ta* and *Te*, roofs of undamaged buildings (c2-c4) were clearly distinguished from the collapsed buildings without correcting threshold values such as *Ev*, and most outlines of undamaged buildings and roads with strong edge elements were distinguished from those of collapsed buildings.

Detection of Areas with Building Damage

The extracted pixels corresponding to the collapsed buildings (c1) were further synthesized to decrease surplus pixels and make areas with building damage easy to identify. This analysis was introduced to calculate the local density of extracted pixels (*Rpx*) as in a previous study (Aoki 2001). *Rpx* is defined as the ratio of the pixels extracted by the four threshold values versus the number of pixels in a window approximating one building size. Windows of 31x31 to 63x63 pixels were selected to be proportional to the resolution of the ground surface. Figure 13 shows the cumulative relative frequency of the training data. Next, a regression line was derived from the same method as used for obtaining the threshold value on edge information, and the threshold value of *Rpx* was defined as the intersection point between the regression line of *Rpx* for the collapsed buildings and the horizontal axis. In all cases of *EvEdTaTe*, *EvEdTa*, and *EvEdTe*, *Rpx* 30% was derived as the threshold value to distinguish between the collapsed buildings and the other imaged objects. A percentage of areas detected as the collapsed buildings in all training data is shown as *Darea* in Table 1. In all cases, correctly detected pixels in the collapsed buildings were more than 90%. However, a small number of pixels for asphalt roads and parking lots (c9), brown exterior walls (c5), and woods (c12) were incorrectly detected by this approach. Therefore, the areas with building damage were estimated using *EvEdTaTe*, because these areas had the least number of incorrect pixels in the three cases. Figures 14 and 15 show the results estimated in this study and the results of ground survey and

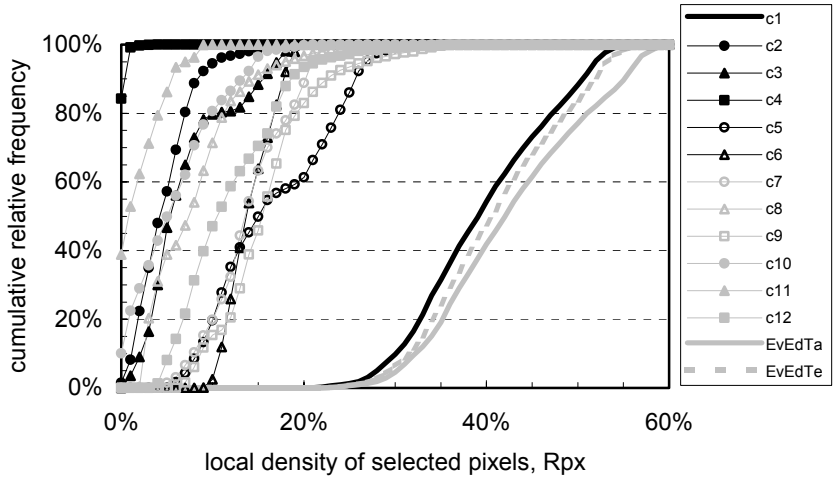

Figure 13. Cumulative relative frequency of *Rpx* for each set of training data. "*EvEdTa*" and "*EvEdTe*" are the distributions of c1 in *EvEdTa* and *EvEdTe*, respectively.

visual inspection (Hasegawa 2000), respectively. The black and white areas in Fig.15 represent the collapsed and the severely damaged buildings, respectively. In the dotted circle, the blue vinyl canvas sheets are covered with parts of the damaged buildings. Most of the building debris was detected correctly, although pedestrian crossings, cars and parts of exterior walls were incorrectly detected as collapsed buildings. Figures 16 and 17 show the result of this method applied to the adjacent image and the distribution of severely damaged buildings due to ground survey and visual inspection, respectively. The distribution of the detected area shown in Figure 16 roughly agreed with that in Figure 17. These results indicate that it may be possible to apply the method based only on edge information from a sample image to several similar images spanning large areas.

Conclusions

The analysis of areas containing collapsed buildings was conducted using panchromatic aerial images taken from a helicopter. The characteristics of collapsed buildings were examined based on edge information of aerial images, such as the variance of edge intensity, the ratio of the predominant edge direction, and two textures based on the co-occurrence matrix of edge intensity. The threshold value was determined by the cumulative relative frequency of the collapsed buildings in terms of edge information, and was combined in order to detect the pixels

Figure 14. Result of estimated areas with building damage based on *EvEdTaTe* and *Rpx*30%.

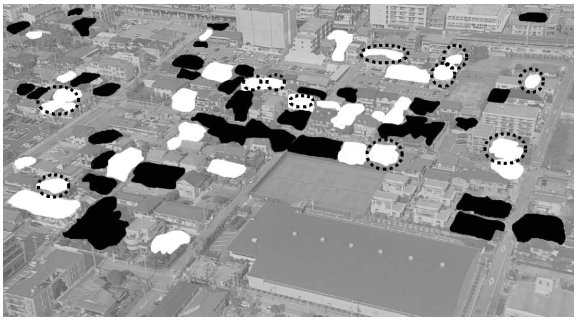

Figure 15. Distributions of collapsed and severely damaged buildings in Fig.14 by ground survey.

Figure 16. Result of application of the threshold value for Fig.14 to an adjacent image.

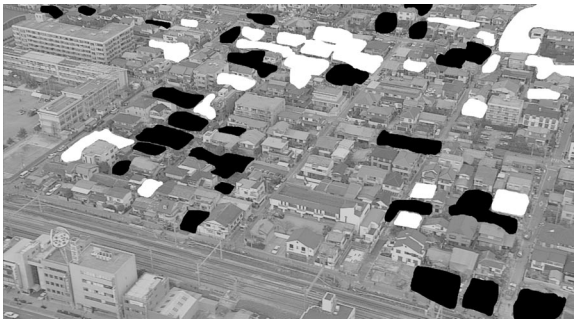

Figure 17. Distributions of collapsed and severely damaged buildings in Fig.16 by ground survey.

representing collapsed buildings. The collapsed areas of buildings were roughly detected by this approach, and these threshold values were applied to an adjacent image. In order to further improve the technique for automated damage detection, we will examine the texture analysis procedure using the co-occurrence matrix, such as appropriate sizes of the matrix, the pixel window, and other textures instead of angular second moment and entropy.

Acknowledgment

We wish to thank the Japan Broadcasting Corporation (NHK) for HDTV images.

References

Aoki, H., M. Matsuoka, and F. Yamazaki (2001). Automated detection of damaged buildings due to earthquakes using aerial HDTV and photographs, *Journal of the Japan Society of Photogrammetry and Remote Sensing,* 40 (4), pp.27-36 (in Japanese).

Gruen, A. (2000). Potential and limitations of highresolution satellite imagery, *The 21st Asian Conference on Remote Sensing,* Keynote address, pp.1-14.

Hasegawa, H., F. Yamazaki, M. Matsuoka, and I. Sekimoto (2000). Determination of building damage due to earthquakes using aerial television images, *The 12th World Conference on Earthquake Engineering,* CD-ROM.

Kosugi, Y., T. Plamen, M. Fukunishi, S. Kakumoto, and T. Doihara (2000). An adaptive nonlinear mapping technique for extracting geographical changes, *Proceedings of GIS2000*, CD-ROM.

Mitomi, H., F. Yamazaki, and M. Matsuoka (2000). Automated detection of building damage due to recent earthquakes using aerial television images, *Proceedings of the 21st Asian Conference on Remote Sensing,* pp.401-406.

Mitomi, H., J. Saita, M. Matsuoka, and F. Yamazaki (2001). Automated damage detection of buildings from aerial television images of the 2001 Gujarat, India earthquake, *IEEE 2001 International Geoscience and Remote Sensing Symposium,* CD-ROM.

Takagi, M., and H. Shimoda (1991). *Handbook of image analysis,* University of Tokyo Press (in Japanese).

Zhang, Q., J. Wang, P. Gong, and P. Shi (2001). Texture analysis for urban spatial pattern study using SPOT imagery, *IEEE 2001 International Geoscience and Remote Sensing Symposium,* CD-ROM.